CrossMark

RESEARCH ARTICLE - EARTH SCIENCES

An Integrated Seismic Interpretation and Rock Physics Attribute Analysis for Pore Fluid Discrimination

Perveiz Khalid[1] · **Nisar Ahmed**[1] · **Azhar Mahmood**[1] ·
Muhammad Ammar Saleem[1] · **Hassan**[1]

Abstract Accurate prediction of subsurface structures, lithologies and pore fluids, is of great interest for petroleum prospecting and reservoir characterization. Seismic reflection data are widely used to mark subsurface structures and lithologies. However, only seismic data are not sufficient to mark fluid heterogeneities present into the pores. Therefore, the use of integrated approach is vital to map subsurface heterogeneities with more accuracy. Based on seismic interpretation, the limestone of Chorgali Formation present in Ratana area of Northern Potwar, Pakistan is interpreted as reservoir rock. Structural interpretation revealed that the study area lies in compressional regime and structures formed are thrust and popups. The reservoir properties such as lithology, porosity, permeability, depositional environments, shale volume, fluid saturation, net pay thickness are determined from petrophysical analysis which confirms that reservoir characteristics of Chorgali limestone are enough to permit hydrocarbon production. Fluid substitution modeling is used to estimate different rock physics attributes such as compressibility, Lame's parameters and their product with density, P to S-wave velocity ratio, impedances and Poisson's ratio are computed as a function of pore fluid type (oil, gas, brine etc.). Sensitivity analysis is performed to derive fluid indicator coefficient which indicates the most appropriate and sensitive rock physics attribute that can be crossplotted to discriminate the rock saturated with different pore fluids (gas/brine/oil).

✉ Perveiz Khalid
perveiz.geo@pu.edu.pk

[1] Institute of Geology, University of the Punjab,
Lahore 54590 Pakistan

1 Introduction

The mapping of subsurface geological structures and lithologies with high level of accuracy is one of the main tasks of seismic interpreters for petroleum prospecting and reservoir characterization [1]. Earlier, only 2D seismic reflection data were used for this purpose; however, the accuracy in results was insufficient and the result was in drilled dry holes [2]. To overcome this problem, an integrated interpretation of geophysical and geological data has been in practice since long. However, this technique is not much appropriate to solve the problems related to fluid discrimination into the pores, reservoir characterization and enhancement of hydrocarbon recovery [3].

In quantitative seismic interpretation, discrimination and identification of pore fluids and their nature in reservoir rocks, is very important and fundamental. Various techniques such as seismic attributes [4], amplitude versus offset analysis [5,6], rock physics modeling [7,8] are widely used to differentiate seismic response of reservoir rocks at various fluid saturation and fluid's nature. Rock physics modeling is used to interpret microscopic and macroscopic pore heterogeneities with much more accuracy [5,6,8]. In quantitative seismic interpretation and rock physics modeling of reservoir intervals, fluid substitution is an important part which provides a tool for fluid identification and quantification of reservoir fluids [5–8]. This is commonly performed by using well-known Gassmann's equation [9]. Many researchers [10–15] have discussed the formulations, strength, limitations and applications of the Gassmann's fluid substitution formula. The main application of fluid substitution is to link petrophysical properties of pore fluids and porous rocks with rock physics properties of a reservoir interval under investigation. Khalid et al. [7] proposed a modified rock physics model to map the seismic properties (seismic velocities and density) of a reser-
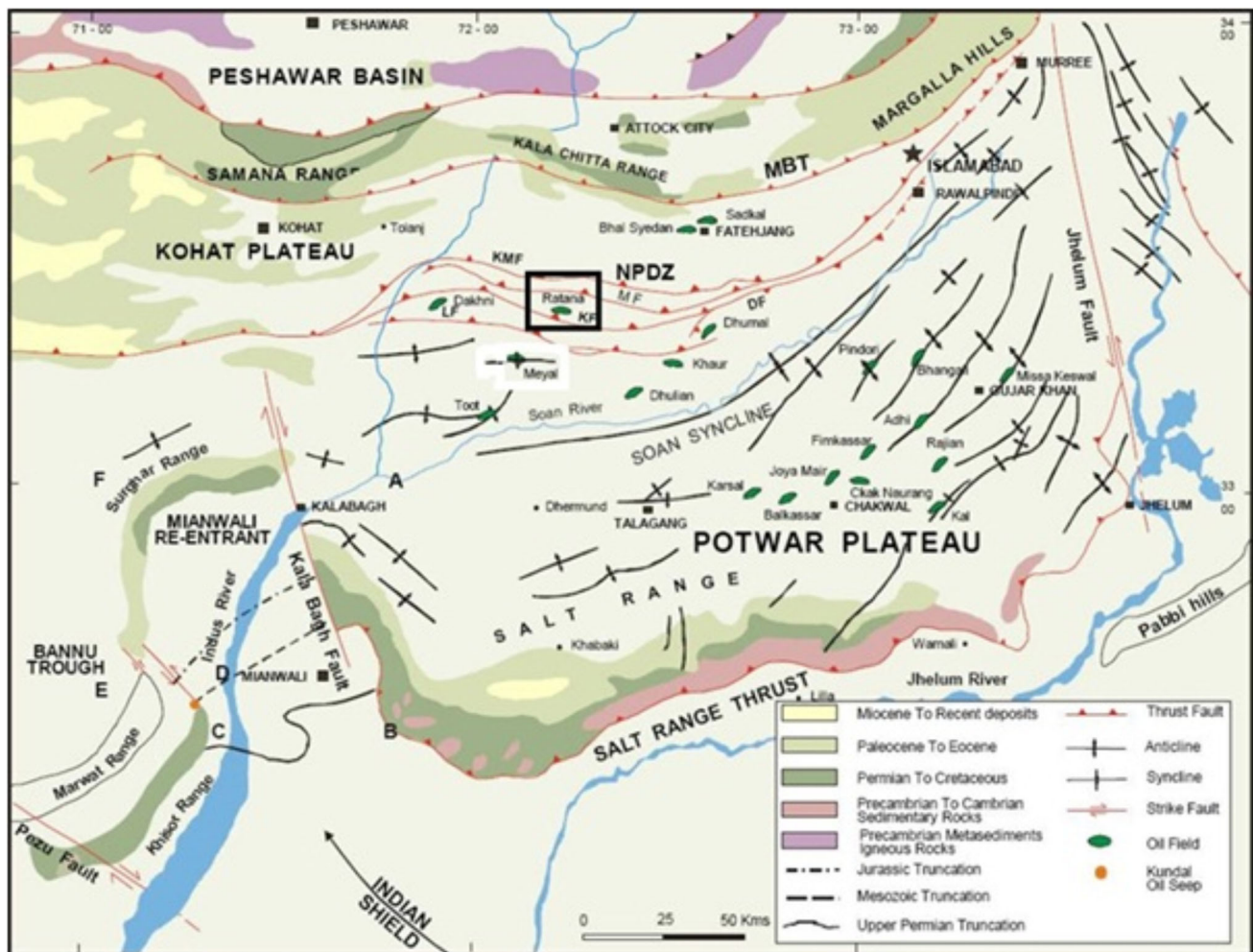
🍃 Springer

Fig. 1 Geological and structural map of Potwar basin along with the highlighted study area (Ratana) (modified from www.gsp.pk.com)

voir interval at in-situ temperature and pressure conditions with proper account of heat and mass transfer effect between the different fluid phases (such as liquid and gas). To differentiate various pore fluids (oil, gas and brine), a large set of rock physics attributes has been generated by using fluid substitution modeling [5,14,16–25].

The Potwar sub-basin of Pakistan (Fig. 1) is highly rich by oil and gas reservoirs [26,27]. Chorgali formation of Eocene age was drilled as potential calcite reservoir in Ratana area of Potwar sub-basin (Fig. 1). Unfortunately, most of the wells in this formation were drilled based on structural seismic interpretation of seismic reflection data and or declared dry or abundant. Less attention was paid on quantitative interpretation of seismic amplitude anomalies related to pore fluid variations. The aim of this work is first to re-interpret the seismic data, correlate it with wireline logs. Then rock physics modeling is applied to interpret fluid related amplitude anomalies, which will be very helpful to asses hydrocarbon potential as well as to map pore scale heterogeneities in fluids. For this

purpose, we computed different rock physics attributes to discriminate seismic response of various pore fluids present in reservoir interval of Chorgali Formation. The sensitivity of these attributes as the best fluid discriminator is determined.

Elastic parameters of rock-fluid composite are fundamental ingredients in sensitivity analysis of fluid indicator coefficient (FIC) [5]. Since most of the rock physics derived attributes and parameters depend directly on the three fundamental seismic properties—seismic velocities (P and S) and density of the rock-fluid composite [28]—therefore, first these fundamental seismic properties are extracted directly from wireline logs are derived from fluid substitution modeling. Then, different rock physics attributes are computed to understand the behavior of reservoir rock saturated with different pore fluids. Gassmann [9] fluid substitution is used to map changes in rock physics parameters at in situ conditions of reservoir rock. To differentiate various pore fluids numerous attributes Poisson's ratio (σ) and combined attributes, e.g., V_P/Vs versus Poisson's ratio, Lame's parameters (μ

and λ) and their product with density (ρ) such as ($\mu^*\rho$) versus ($\lambda^*\rho$), the difference in saturated rock bulk modulus and shear modulus ($K_{sat} - \mu$) versus ($\mu^*\rho$), I_P (P-wave acoustic impedance) versus I_S (S-wave acoustic impedance), and I_S versus ($I_P - I_S$) with respect 100 % water saturation, 100 % oil saturation and 100 % gas saturation are analyzed in the limestone interval of Chorgali Formation. The appropriate pairs of these attributes are crossplotted to interpret and discriminate various pore fluids.

2 Geology of the Area

The study area is located in western part of North Potwar Deformed Zone (NPDZ), about 100 km southwest of Islamabad, Pakistan. The Potwar sub-basin is located in the western foothills of Himalayas [29]. Geological and structural map of Potwar basin showing the location of Ratana area is shown in Fig. 1. The Potwar sub-basin is one of the oldest oil provinces of the world, where the first commercial discovery was made in 1914 at Khaur. The Potwar sub-basin has experienced severe deformation during Himalayan orogeny in Pliocene to Middle Pleistocene due to which the surface geological features often mismatch with the subsurface structural geometry. This disharmony between the subsurface and surface structure suggests the presence of detachment zone in the younger molasses deposits [30]. Subsurface structural analysis of seismic data represents that Ratana area is a large salt cored thrust bounded complex structures. The whole research area is affected by compressional regime. Major structures found in the area are thrusts; tight anticlines and pop up structures which are clearly marked on the interpreted seismic section as given in Fig. 2. Previous studies and stratigraphy of the area show that rocks from Precambrian to quaternary age are present in Potwar sub-basin [26,29,30]. Based on seismic interpretation, Ratana-02 well was drilled on seismic line NP86-04 in limestone of Chorgali Formation, which is the reservoir rock in study area. For better visualization of subsurface style of the study area, the seismic data have been converted into depth domain. Seismic velocities extracted from sonic log are used for depth conversion. Figure 3 shows the 3D depth structural map of Chorgali Formation that demonstrates the subsurface complexities of whole block more transparently.

3 Methodology Work Flow and Data Resources

The petrophysical analysis of well logs and rock physics modeling of different physical properties is a fundamental step of any exploration and production strategy. For the robust integrated interpretation of seismic data and for the construction of an appropriate model, well understanding of physical properties of a reservoir rock is very important. We have used the 2D seismic reflection data and a complete suite of wireline logs run in the Ratana-02 well. The petrophysical log comprises caliper, spectral gamma ray, resistivity, sonic, bulk density, neutron porosity etc. Total 20 core plugs collected in reservoir interval of Chorgali Formation were also analyzed for quality check and calibration of the results. However before initiating the study, the quality checks have been made on the required data set. Before performing the rock physics modeling and calculating rock physics attributes as function of pore fluids (oil, gas and brine), we have executed the petrophysical study in the reservoir zone and derived the inputs (porosity, volume of clay, major lithology, fluids saturation, seismic velocities and bulk density etc.) required for further fluid substitution and rock physics modeling.

Fluid substitution analysis (FSA) of in-situ reservoir pore fluids is helpful for sensitivity analysis of different rock physic attributes which make easy to distinguish fluid nature and its quantity in reservoirs. FSA provides the understanding and interprets how seismic parameters depend on pore fluid (water, oil or gas) saturation. Gassmann's equation [9] is used for fluid substitution analysis, and it helps to compute the saturated rock bulk modulus as function of pore fluids (oil, gas and brine) at known saturation of pore fluid. The Gassmann's equation is given below.

$$K_{sat} = \frac{\left[1 - \frac{K_{frame}}{K_{matrix}}\right]^2}{\frac{\phi}{K_{fl}} + \frac{(1-\phi)}{K_{matrix}} - \frac{K_{frame}}{K_{matrix}^2}} \tag{1}$$

where K_{sat}, K_{matrix}, K_{fl} and K_{frame} are the bulk moduli of saturated rock, rock matrix, pore fluid and rock frame (dry rock skeleton), respectively, and ϕ is the effective porosity of reservoir interval derived from sonic (DT) log. Since sonic log and density log data are available, therefore bulk modulus of saturated rock interval can be derived directly from logs by using $K_{sat} = V_P^2\rho - 4/3\mu$ (here μ is shear modulus of reservoir interval). The value of K_{matrix} is opted according to the lithology of reservoir interval. From logs interpretation, the reservoir interval is limestone, which is calcite dominant; therefore, K_{matrix} is computed using Voigt–Reuss–Hill (VRH) average methods [31–34]. Empirical relations are used to compute dry rock modulus (K_{frame}) as a function of porosity [35]. The modulus of the mixture of fluid (K_{fl}) can be computed using Wood's average equation [36]. The mathematical relations for K_{matrix} and K_{fl} are

$$K_{matrix} = \frac{1}{2}\sum_{i=1}^{n} f_i K_i \tag{2}$$

$$K_{fl} = \left[\frac{S_w}{K_w} + \frac{1 - S_{hyd}}{K_{hyd}}\right]^{-1} \tag{3}$$
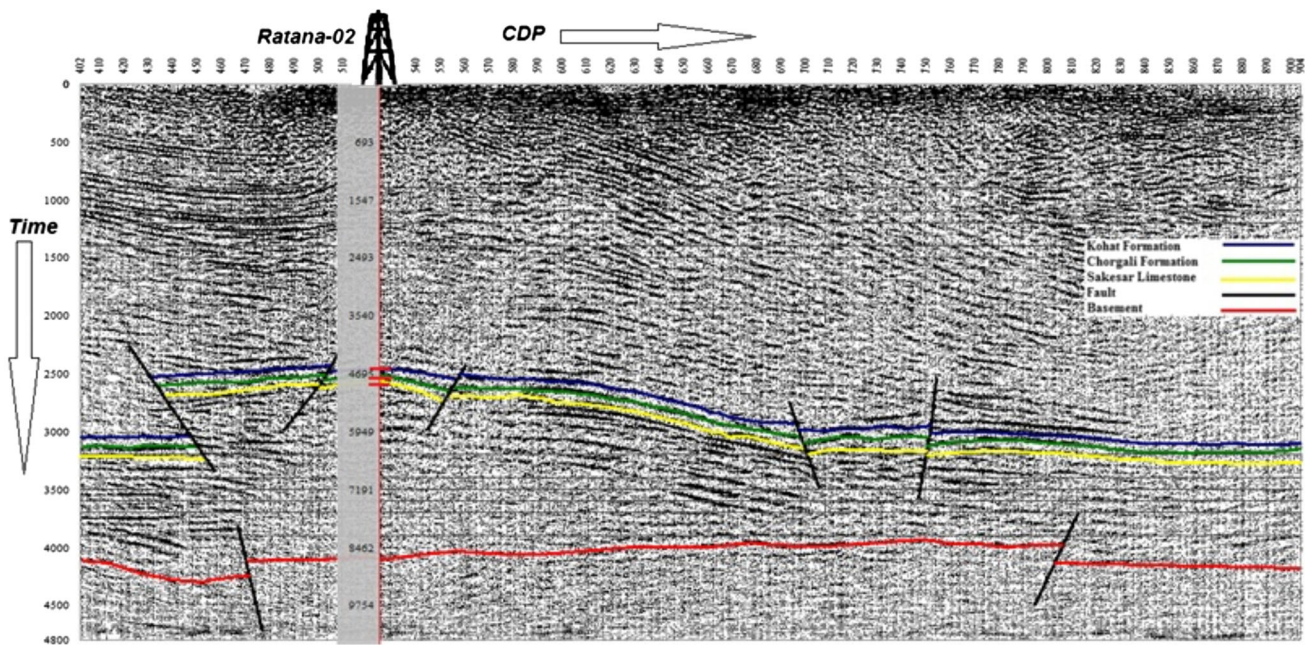
Fig. 2 Interpreted time section of seismic line NP86-04 showing major horizons marked with *different colours*; Basement (*red*), Sakesar limestone (*yellow*), Chorgali formation (*green*) and Kohat formation (*blue*). The well location of Ratana-02 is also shown

Fig. 3 3D depth contour map of Chorgali Formation, which is the reservoir rock in the study area. The map showing synclinal and anticlinal structures present in the area
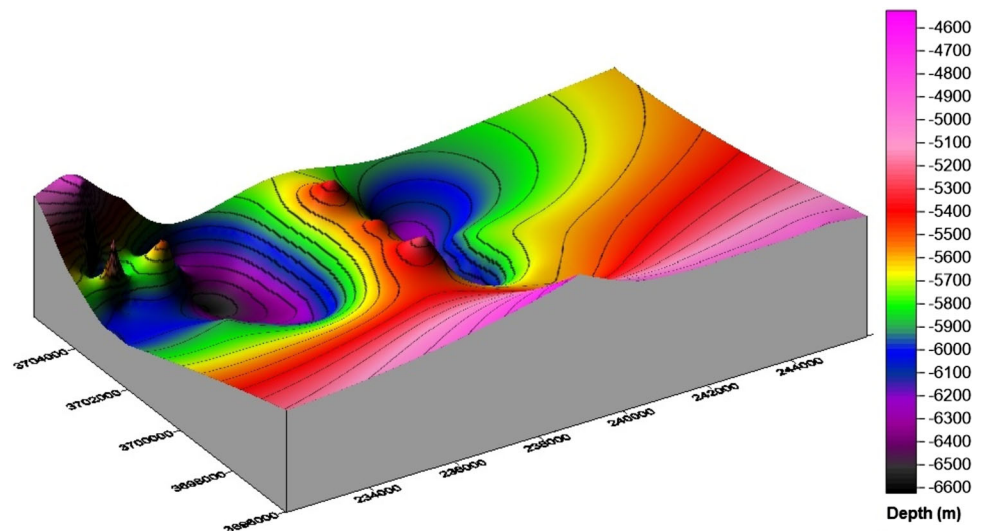
In the Eq. (2), f and K are the volume fraction and bulk modulus of minerals present in the reservoir rocks, while the subscript i describes the number of minerals present. In the Eq. (3) of fluid bulk modulus, K_w and K_{hyd} are the bulk moduli of water and hydrocarbon whereas S_w and S_{hyd} are the volume fractions of brine and hydrocarbons (oil/gas) phases, respectively. Since the shear modulus is independent of pore fluid, therefore, in Gassmann's fluid substitution it is assumed that the saturated rock shear modulus (μ) is equal to dry rock shear modulus (μ_{dry}) i.e., $\mu_{sat} = \mu_{dry}$ which is calculated by following equation.

$$\mu = V_S^2 \times \rho \tag{4}$$

In the presence of shear log data, shear modulus can be derived directly from shear log by using the above relationship.

Finally, P- and S-wave velocities (V_P and V_S) are calculated by using the relations.

$$V_P = \sqrt{\frac{K_{sat} + \frac{4}{3}\mu}{\rho}} \tag{5}$$

$$V_S = \sqrt{\frac{\mu}{\rho}} \tag{6}$$

where bulk density (ρ) can be find out as

$$\rho = (1 - \phi)\rho_{\text{matrix}} + \phi\rho_{\text{fluid}} \qquad (7)$$

whereas ρ_{matrix} and ρ_{fluid} are the density of rock matrix and pore fluids, respectively. All other rock physics attributes such as Lame's parameters (λ and μ), P- and S-wave acoustic impedances, Poisson's ratio, V_P/V_S ratio $K_{\text{sat}} - \mu$ are further derived by using seismic velocities calculated by Gassmann's fluid substitution analysis. The P-wave acoustic impedance (I_P) and S-wave acoustic impedance (I_S) are calculated by using the following simple formulas:

$$I_P = V_P\rho \qquad (8a)$$
$$I_S = V_S\rho. \qquad (8b)$$

For λ and σ , these relationships are used [37]

$$\lambda = K_{\text{sat}} - 2/3\mu \qquad (9a)$$
$$\sigma = \frac{(V_P/V_S)^2 - 2}{2[(V_P/V_S)^2 - 1]} \qquad (9b)$$

We have performed the FSA in the reservoir intervals (4700–4750 m) of Ratan-02 well by using the wireline logs data. The input parameters required for FSA are given n Table 1. All the rock physics attributes are computed by considering the reservoir rock when it is fully saturated with pore fluids (oil, gas and brine). Finally we have cross plotted the appropriate attribute to discriminate rock saturated with oil, gas and brine. The visual relationship between two or more seismic attributes derived from fluid substitution modeling is demonstrated by preparation of crossplots. This visualization is quite helpful to discriminate various pore fluids in reservoir rock. Crossplotting appropriate pairs of attributes so that various pore fluids generally cluster together that allows for straightforward understanding.

The FIC plot effectively used to check which rock physics attribute is best to discriminate pore fluids. The FIC can be described as the difference between the mean values of any rock physics parameter at reservoir interval saturated with 100 % brine (m_b) and reservoir interval saturated with 100 % hydrocarbon (m_h) divided by the standard deviation ($s \cdot t_h$) of that rock physics parameter in the whole reservoir interval saturated with 100 % hydrocarbon. The mathematical relationship for the computation of FIC is given as [37]:

$$\text{FIC} = \frac{m_b - m_h}{s \cdot t_h} \qquad (10)$$

Here m stands for mean value of any rock physics parameter under investigation.

The sensitivity of fluids is very good in younger or poorly consolidated rocks; therefore, the simple seismic attributes such as acoustic impedances are sufficient to discriminate

Table 1 Input parameters derived from wireline logs data and laboratory measurements used for performing fluid substitution analysis

	Well Ratan-02
Reservoir interval (m)	4700–4750
Average reservoir temperature (°C)	153
Average effective pressure (MPa)	48
Average porosity (%)	10.52
Average shale volume (%)	11.48
Specific gravity of gas	0.6
In situ gas density (g/cm³)	0.10
In situ oil density(g/cm³)	0.74
Bulk modulus of gas (GPa)	0.1073
Bulk modulus of oil (GPa)	1.12
Insitu density of brine (g/cm³)	1.155
Bulk modulus of brine (GPa)	3.44
Bulk modulus of calcite(GPa)	76
Bulk modulus of clay (GPa)	21
Density of calcite (g/cm³)	2.71
Density of clay (g/cm³)	1.8
In situ P-wave velocity for brine (m/s)	1727.44
In situ P-wave velocity for oil (m/s)	1202

various fluids. However, in older or highly consolidated sedimentary sequences as in this case, the use of combination of seismic attributes is mandatory for the optimization of fluid discrimination procedure.

4 Results

The quantitative workflow stated above is implemented on the real data set taken from Ratana area, Potwar Basin, Pakistan (Fig. 1).

4.1 Petrophysical Analysis

After identification of different lithological units from seismic interpretation, detailed petrophysical analysis is performed. In seismic interpretation, four major horizons named Kohat Formation, Chorgali Formation, Sakesar Limestone and basement rocks are marked (Fig. 2).

Robust petrophysical analysis, based on well logs and core plugs, is essential to mark and confirm reservoir zone. Petrophysical interpretation of wireline logs confirms that Chorgali Formation is a reservoir rock. In Fig. 4 the results of logs interpretations within the interval of Chorgali Formation (4700–4750 m) have been described. Various logs such as spectral gamma ray (SGR), density (RHOB), sonic (DT), resistivity (LLD) and porosity log (PHI) are interpreted and plotted along with water saturation curve (SWu) and vol-
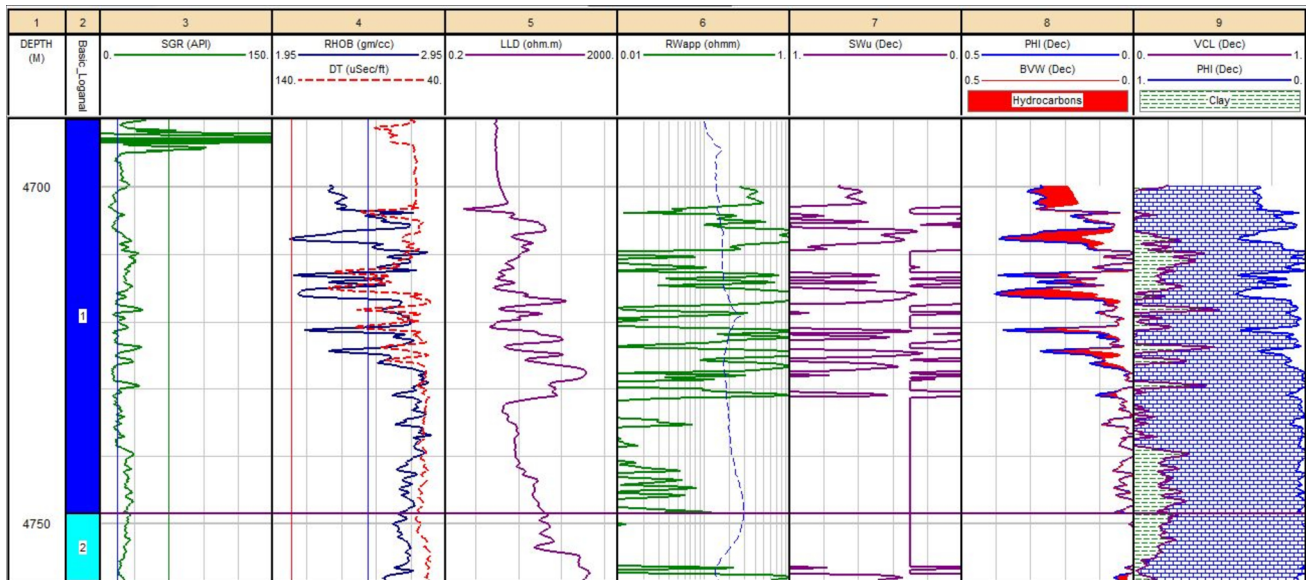
Fig. 4 Detailed petrophysical analysis and wireline log interpretation of Chorgali Formation encountered in Ratana-02 well at a depth interval of 4700–4750 m. Based on volume of clay, water saturation and porosity, pay zone is marked with *red colour* in the depth range of 4700–4730 m

ume of clay (VCL) as shown in Fig. 4. The SGR response within the reservoir zone is very low (API ∼ 15), which indicates that it has very small amount of clays (VCL ∼ 11.4 %) and dominant lithology is calcite-rich carbonate rocks. The hydrocarbons have much higher resistivity values and small density as compare to water or brine. Therefore, the reservoir interval with relatively smaller density and water saturation values but higher porosities and resistivity are marked as net pay zones (containing hydrocarbons marked with red colour) are shown in Fig. 4. The petrophysical analysis reveals that the average porosity within the reservoir intervals is about 0.11 and water saturation is 0.40.

4.2 Fluid Indicator Coefficients

Fluid indicator coefficients (FICs) have the ability to calculate the attributes values universally for excellent discrimination between different fluids [5]. Higher the values of FIC means good differentiation between the pore fluids. To analyze the sensitivity of each rock physics attribute for different pore fluid types, various FICs are computed for numerous rock physics attributes of reservoir fluids (gas and oil) with respect to brine by using the equations given in previous section.

Table 2 summarizes the numerical results of FICs for various attributes such as saturated rock bulk modulus (K_{sat}), P-wave to S-wave velocity ratio (V_P/V_S), Poisson's ratio (σ), Lame's parameter (λ), P-wave acoustic impedance (I_P), S-wave acoustic impedance (I_S), difference in bulk and shear moduli ($K_{sat} - \mu$), $\lambda^*\rho$, $\mu^*\rho$ etc. for both cases when the reservoir interval is fully saturated with oil and gas. These

attributes are plotted in Fig. 5a for oil-saturated and gas-saturated reservoir interval. The value of each indicator is higher for gas-saturated interval in comparison with oil saturated except λ. It is clear from figure that the values of FIC for $\lambda^*\rho$, λ, $K_{sat} - \mu$, K_{sat} and $I_P - I_S$ are higher as compared to other attributes. However, the relative difference between these attributes for oil and gas cases is not much prominent (Fig. 5b). The relative difference in $\mu^*\rho$ for oil- and gas-saturated intervals is more than 60 %, which make it a useful attribute for oil and gas discrimination. Similarly, the relative difference in shear wave impedance and acoustic wave impedance for oil and gas are also quite obvious.

4.3 Crossplot Analysis of Rock Physics Attributes for Fluid's Discrimination

In this section we have crossplotted the suitable pairs of above-prescribed rock physics attributes so that to analyze which combination is excellent discriminator. Different rock physics attributes like V_P/V_S, σ, $\mu^*\rho$, $\lambda^*\rho$, $K_{sat} - \mu$, I_P and I_S are applied to determine the rock properties which are effectively discriminate pore fluids in the prospective reservoir intervals. V_P/V_S ratio is a good tool for fluid identification [38]. It is observed that P-wave velocity decreases and S-wave velocity increases with increase in hydrocarbon saturation, which makes V_P/V_S ratio more sensitive fluid indicator. In Fig. 6, Poisson's ratio and V_P/V_S ratio is crossplotted against each other for carbonate reservoir interval, when it is fully saturated with oil, gas and brine. Clearly, both parameters have much higher values for all samples of brine-saturated interval. Both σ and V_P/V_S ratio has much

Table 2 Fluid indicator coefficients (FICs) calculated for different rock physics attributes for oil and gas-saturated rocks with respect to brine. Higher FIC means that more excellent discriminator the hydrocarbon fluids from non-hydrocarbon fluids

	K_{sat}	V_P/V_S	σ	λ	$K_{sat} - G$	$G*\rho$	$\lambda*\rho$	I_P	I_S	$I_P - I_S$
Mean Brine	42.636	1.707	0.217	21.976	11.646	77.448	54.370	14.412	8.545	5.668
SD	10.600	0.224	0.067	6.120	6.835	32.401	17.200	2.701	2.109	0.820
Mean _oil	36.607	1.634	0.182	15.947	5.616	76.278	38.707	13.551	8.470	5.081
SD	9.605	0.176	0.069	5.336	6.578	32.644	14.493	2.766	2.133	0.797
FIC for oil	0.628	0.412	0.515	1.130	0.917	0.036	1.081	0.239	0.035	0.736
Mean _gas	34.754	1.615	0.155	14.094	3.764	74.555	33.179	13.189	8.350	4.839
SD	10.548	0.223	0.106	7.284	8.405	33.090	18.976	2.891	2.168	1.133
FIC for gas	0.747	0.410	0.589	1.082	0.938	0.087	1.117	0.354	0.090	0.731

Fig. 5 **a** Fluid indicator coefficients (FICs) for oil- and gas-saturated reservoir intervals with respect to brine-saturated rock and **b** the relative difference between oil-saturated and gas-saturated fluid indicator coefficients. The input parameters used in the computation of FIC are given in Table 1. Equation (10) is used in the computation of FIC
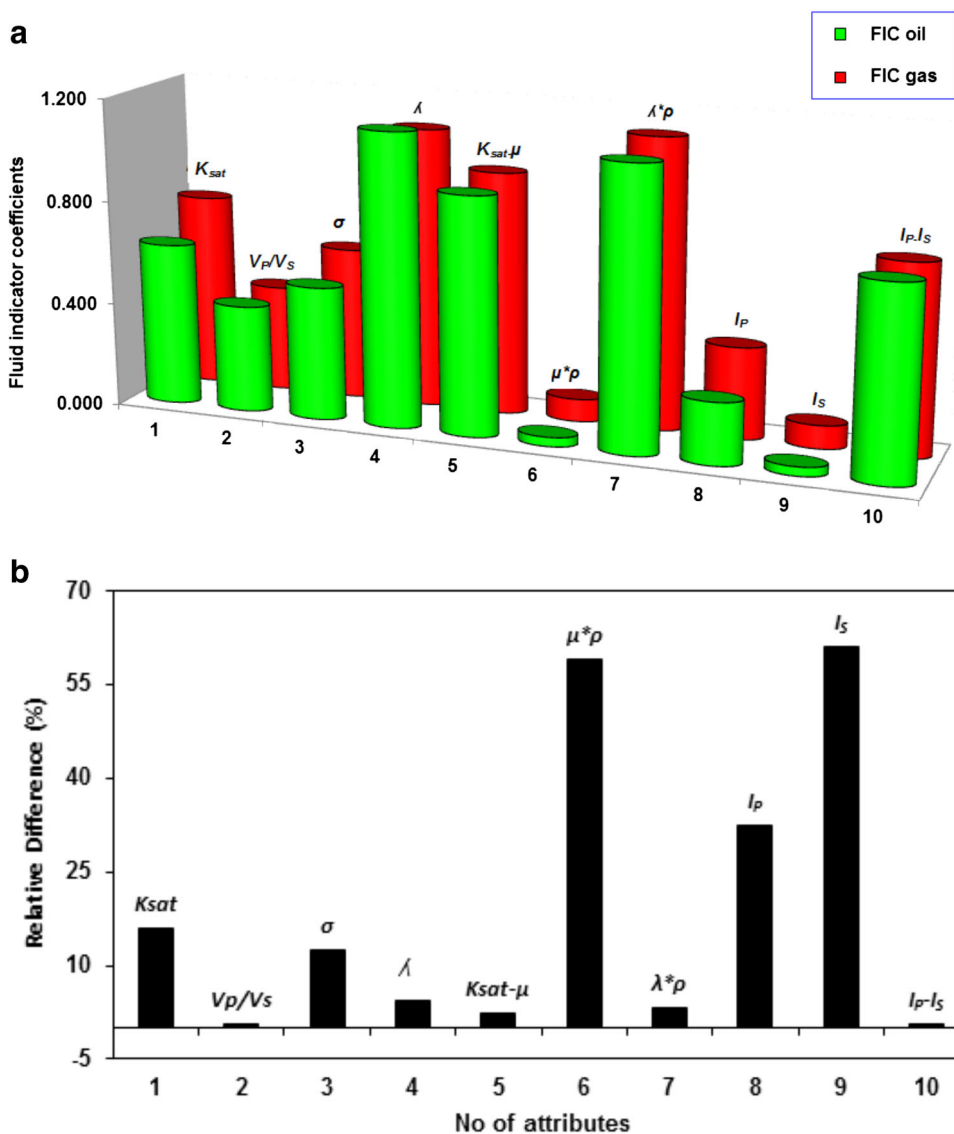
lower value for gas/oil reservoirs as compared to brine. The relative difference between their values is less than 5 %. It is because P-wave velocity decreases with hydrocarbon saturation, while S-wave velocity increases, which causes to decrease their ratio. Poisson's ratio is directly dependent on V_P/V_S also reduces with hydrocarbons saturation. In Fig. 6, an excellent discrimination can be observed between brine and hydrocarbons facies along the both axis; however, a small
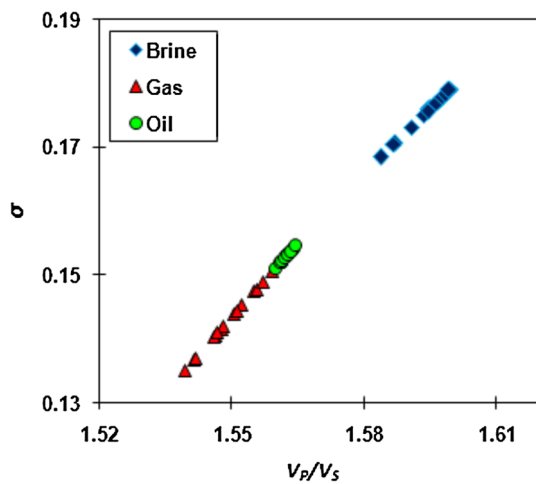
Fig. 6 Crossplot between Poisson's ratio and V_P/V_S ratio of reservoir interval saturated with gas, oil and brine. A linear trend is present between these parameters. Brine-saturated interval has higher values than oil- and gas-saturated intervals and is clearly distinguishable

Fig. 7 Crossplot analysis of $\lambda * \rho$ and $\mu * \rho$ shows that $\lambda * \rho$ is more robust attribute. The values of these attributes for oil-, gas- and brine-saturated intervals fall in three different clearly distinguishable intervals of values. Brine-saturated interval has highest values of these attributes. Almost linear trend is notable between $\lambda * \rho$ and $\mu * \rho$

overlapping is present between oil and gas cases in some samples.

After computing the seismic velocities and bulk density as a function of pore fluids, elastic parameters (λ and μ) of fluid saturated rock are determined by inverting the seismic velocities. Lamé's elastic parameters λ and μ and their products with density (also called LMR method: L for Lambda, M for Mu and R for Rho; here λ represents Lambda, μ is for Mu and ρ for Rho as introduced by [20]) might be a useful tool for fluid discrimination [20]. To check their insight response to pore fluids in carbonate reservoir, the combination of λ and μ with bulk density (by scalar product) are crossplotted against each other. Figure 7 demonstrates the crossplot between $\lambda * \rho$ (Lambda-Rho) and $\mu * \rho$ (Mu-Rho) for reservoir pore fluids (oil, gas and brine). There is a good separation between gas, oil and brine-saturated rocks in direction of $\lambda * \rho$ as compared to $\mu * \rho$. A little bit overlapping exists along the $\mu * \rho$ axis because of the insensitivity of shear modulus to pore fluids and bulk density drops more rapidly when reservoir is fully saturated with gas, hence plays an important role in separation of pore fluids. In the Fig. 5, where FIC are plotted $\lambda * \rho$ has higher value shows more effective rock physics attribute for fluids discrimination.

The difference between saturated bulk modulus and shear modulus ($K_{sat} - \mu$) and the product of shear modulus and density ($\mu * \rho$) is also very effective fluid indicator that is not only helpful to discriminate the hydrocarbon facies (oil and gas) but also them to non-reservoir rocks. These attributes are plotted in Fig. 8. These attributes have much higher values for brine-saturated intervals. However, for gas-saturated interval, their values are lowest and are clearly distinguishable from oil and brine-saturated intervals. The acoustic and shear wave impedances were also used as fluid discriminator
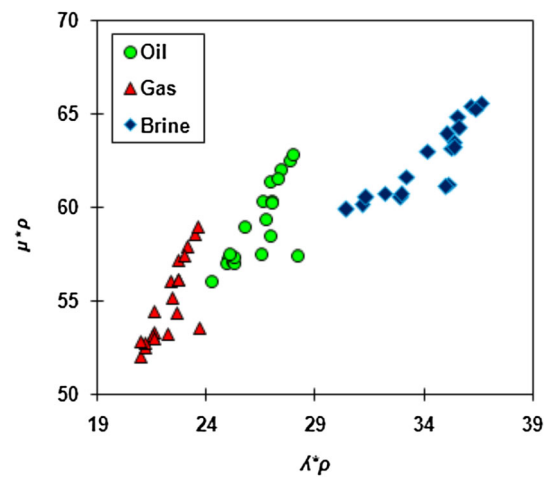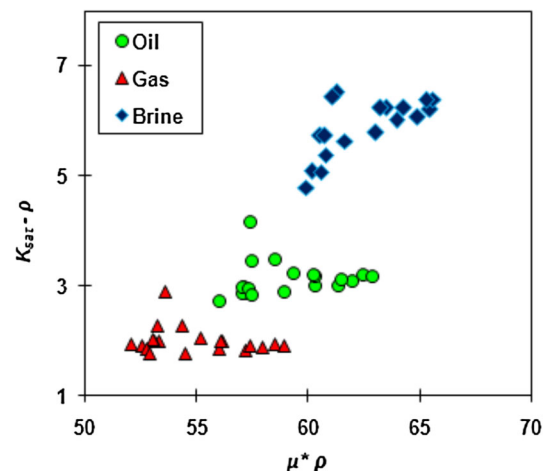

Fig. 8 The crossplot between $K_{sat} - \mu$ and $\mu * \rho$ for brine, oil and gas-saturated reservoir intervals. All input parameters used for the computation of these parameters are given in Table 1. The reservoir fluids discrimination ability is more in case of $K_{sat} - \mu$

[2]. We have tested these attributes as well and the P-wave acoustic impedance (I_P) is crossplotted with S-wave acoustic impedance (I_S) in Fig. 9 for reservoir interval saturated with brine, oil and gas respectively. The I_P and I_S values overlap for brine and oil; and for oil and gas thus, these attributes have less ability to separate the pore fluids and not clearly separate out the oil, gas and brine facies. However, a linear relationship exists between acoustic and shear impedances for oil, gas and brine facies.
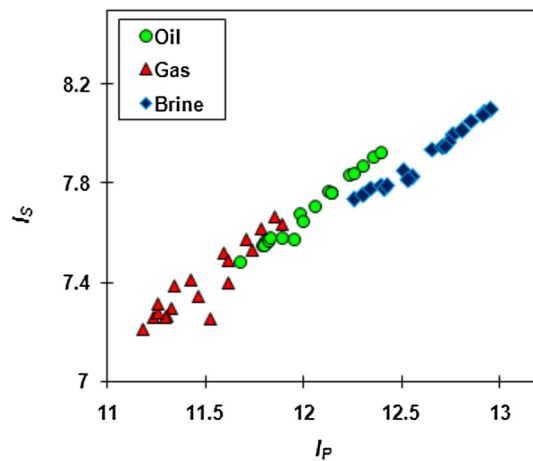
Fig. 9 Crossplot between (I_P) and (I_S) showing a linear trend between acoustic and shear impedances for oil-, gas- and brine-saturated reservoir intervals. See Table 1 for all input values to compute these attributes. A small overlapping exists along the both axis

5 Conclusions

Seismic interpretation is very important to delineate the subsurface structures that can accumulate treasures of oil and gas reserves for us. Based on seismic structural interpretation, it is concluded that pop up and thrusts are present in this area that are suitable traps for subsurface accumulation of hydrocarbons. Detailed petrophysical analysis has further confirmed that Chorgali Formation possesses complete petrophysical reservoir characteristics to be a hydrocarbon producing zone. Different rock physics attributes derived by using Gassmann's fluid substitution analysis are crossplotted to discriminate different pore fluids present within the reservoir pores. The results reveal that the use of integrated seismic attributes is more effective for fluid discrimination purposes. Fluid indicator coefficient value shows that λ is most sensitive and one of the important fluid indicators that help to discriminate brine and hydrocarbon saturated facies. However, for differentiation of oil-saturated and gas-saturated the use of $\mu^*\rho$, P-wave acoustic impedance and S-wave acoustic impedance is more useful.

References

1. Ahmed, N.; Ali, S.H.; Khalid, P.: Subsurface structural mapping of eastern Potwar, Pakistan: an application of seismic reflection. Geol. Bull. Punj. Univ. **47**, 1–12 (2012)

2. Khalid, P.; Ghazi, S.: Discrimination of fizz water and gas reservoir by AVO analysis: a modified approach. Acta Geod. Geophys. **48**, 347–361 (2013)

3. Avseth, P.; Mukerji, T.; Mavko, G.: Quantitative Seismic Interpretation: Applying Rock Physics Tools to Reduce Interpretation Risk. Cambridge University Press, Cambridge (2005)

4. González, E.F.: Physical and quantitative interpretation of seismic attributes for rocks and fluids identification. Ph.D. Thesis, Stanford University (2006)

5. Khalid, P.; Ahmed, N; Khan, K.A.; Naeem, M.: AVO-derived attributes to differentiate reservoir facies from non-reservoirs facies and fluid discrimination in Penobscot area, Nova Scotia. Geosci. J. (2014) doi:10.1007/s12303-014-0048-0

6. Ahmed, N.; Khalid, P.; Anwar, A.W.; Ghazi, S.: AVO forward modeling and attributes analysis for fluid's identification: a case study. Acta Geod. Geophys. (2015). doi:10.1007/s40328-014-0097-x

7. Khalid, P.; Brosta, D.; Nichita, D.V.; Blanco, J.: A modified rock physics model for analysis of seismic signatures of low gas-saturated rocks. Arab. J. Geosci. **7**, 3281–3295 (2014)

8. Ahmed, N.; Khalid, P.; Anwar, A.W.: Rock physics modelling to assess the impact of spatial distribution pattern of pore fluid and clay contents on acoustic signatures of partially-saturated reservoirs. Acta Geod. Geophys. (2015). doi:10.1007/s40328-015-0101-0

9. Gassmann, F.: Uber die Elastizitatporoser Medien. Vierteljahrsschr. Natforsch. Ges. Zür. **96**, 1–23 (1951)

10. Batzle, M.L.; Wang, Z.: Seismic properties of pore fluids. Geophysics **64**, 1396–1408 (1992)

11. Berryman, J.G.: Tutorial: origin of Gassmann's equation. Geophysics **64**, 1627–1629 (1999)

12. Wang, Z.: Fundamental of seismic rock physics. Geophysics **66**, 398–412 (2001)

13. Smith, T.M.; Sondergeld, C.H.; Rai, C.S.: Gassmann fluid substitution: a tutorial. Geophysics **68**, 430–440 (2003)

14. Russell, B.H.; Hedlin, K.; Hilterman, F.J.; Lines, L.R.: Fluid-property discrimination with AVO: a Biot–Gassmann perspective. Geophysics **68**, 29–39 (2003)

15. Han, D.; Batzle, M.L.: Gassmann's equation and fluid-saturation effects on seismic velocities. Geophysics **69**, 398–405 (2004)

16. Smith, G.C.; Gidlow, P.M.: Weighted stacking for rock property estimation and detection of gas. Geophys. Prospect. **35**, 993–1014 (1987)

17. Verm, R.; Hilterman, F.: Lithology color-coded seismic sections: the calibration of AVO crossplotting to rock properties. Lead. Edge **14**, 847–853 (1995)

18. Goodway, W.; Chen, T.; Downton, J.: Improved AVO fluid detection and lithology discrimination using Lamé parameters: $\lambda\rho$, $\mu\rho$ and λ/μ fluid stack from P and S inversions. In: 67thAnnual International Meeting, Society of Exploration Geophysics, Expanded Abstracts, pp. 148–151 (1997)

19. Castagna, J.P.; Swan, H.S.; Foster, D.J.: Framework for the interpretation of AVO intercept and gradient. Geophysics **63**, 948–956 (1998)

20. Chen, T.; Goodway, B.; Zhang, W.; Potocki, D.; Calow, B.; and Gray, D.: Integrating geophysics, geology and petrophysics: A 3D seismic AVO and borehole/logging case study. In: 68th Annual International Meeting, Society of Exploration Geophysics, Expanded Abstracts, pp. 615–618 (1998)

21. Connolly, P.: Elastic impedance. Lead. Edge **18**, 438–452 (1999)

22. Hedlin, K.: Pore space modulus and extraction using AVO. In: 70th Annual International Meeting, Society of Exploration Geophysics, Expanded Abstracts, pp. 170–173 (2000)

23. Berryman, J.G.; Berge, P.A.; Bonner, B.P.: Estimating rock porosity and fluid saturation using only seismic velocities. Geophysics **67**, 391–404 (2002)

24. Quakenbush, M.; Shang, B.; Tuttle, C.: Poisson impedance. Lead. Edge **25**, 128–138 (2006)

25. Pengyuan, S.; Xiuli, L.; Yanpeng, L.; Yuanyuan, Y.; Haifeng, C.: Elastic parameter AVO approximation and their applications. In: Annual International Meeting, Society of Exploration Geophysics, Expanded Abstract, pp. 523–527 (2008)

26. Ghazi, S.; Aziz, T.; Khalid, P.; Sahraeyan, M.: Petroleum Play analysis of the Jurassic sequence, Meyal Oil-field, Potwar Basin, Pakistan. J. Geol. Soc. India **84**, 727–738 (2015)

27. Khalid, P.; Yasin, Q.; Sohail, G.M.D.; Kashif J.M.: Integrating core and wireline log data to evaluate porosity of Jurassic formations of Injra-1 and Nuryal-2 wells, Western Potwar, Pakistan. J. Geol. Soc. India (2015, accepted)

28. Khalid, P.: Effects on seismic properties of thermoelastic relaxation and liquid/vapor phase transition. Ph.D. Thesis, University of Pau (2011)

29. Kazmi, A.; Jan, M.: Geology and Tectonics of Pakistan. Karachi Graphic Publishers, Karachi (1997)

30. Siddiqui, S.U.; Elahi, N.;Siddiqui, A.J.: A case history: case histories of eight oil and gas fields in Pakistan. Published in proceedings of Pakistan petroleum convention (1998)

31. Voigt, W.: Lehrbuch der Kristallphysik. Leipzig, Teubner (1910)

32. Reuss, A.: Berechnung der fliessgrense von mischkristallen auf grund der plastizitatbedingung fur einkristalle. Z. Ange-Wandte Math. Mech. **9**, 49–58 (1929)

33. Hill, R.: The elastic behavior of a crystalline aggregate. Proc. Phys. Soc. Lond. Ser. A **65**, 349–354 (1952)

34. Mavko, G.; Mukerji, T.; Dvorkin, J.: The Rock Physics Handbook: Tools for Seismic Analysis of Porous Media, 2nd edn. Cambridge University Press, Cambridge (2009)

35. Murphy, W.; Reischer, A.; Hsu, K.: Modulus decomposition of compressional and shear velocities in sand bodies. Geophysics **58**, 227–239 (1993)

36. Wood, A.B.: A Textbook of Sound. G. Bell and sons, London (1941)

37. Dillon, L.; Schwedersky, G.; Vasquez, G.; Velloso, R.; Nunes, C.: A multi-scale DHI elastic attributes evaluation. Lead. Edge **22**, 1024–1029 (2003)

38. Hamada, G.M.: Reservoir fluids identification using VP/VS ratio. Oil Gas Sci. Technol. **59**, 649–654 (2004)